Modeling the Vulcanization of Rubbers in an Oscillating Bicone Cell

JULIO A. DEIBER,* RAÚL A. BORTOLOZZI, and MARTA B. PEIROTTI

Instituto de Desarrollo Tecnológico para la Industria Química, INTEC, Güemes 3450, 3000 Santa Fe, Argentina

SYNOPSIS

This work studies the evolution of dynamic rheometric functions (dynamic viscosity $\eta'(\omega)$ and storage modulus $G'(\omega)$) with the degree of vulcanization and temperature of well-characterized SBR and NBR compounds. Experiments are carried out in an oscillating bicone cell, and results are well fitted through a model that considers flow kinematics, heat transfer, curing kinetics, and rheological functions. It is possible to quantify the model parameters and to understand better the evolution of filled rubber compounds toward crosslinked networks or vulcanizates. Conclusions are also obtained on the interplay between rheological functions and molecular parameters (average molecular weight and polydispersity). Experimental evaluations of the ratios between oscillating torques, at different times of the curing process, correlate directly with changes in rheological properties of the samples studied. © 1995 John Wiley & Sons, Inc.

INTRODUCTION

The curve obtained by monitoring the torque in an oscillating rheometric cell, during the cure of rubber compounds, is valuable to control the quality of final products. It has been used for many years and well-qualified commercial apparatus can be found for this purpose. ASTM norms present a clear procedure to carry out the test (see, e.g., Norm D 2084). This curve has important information on rheological properties when thermal and chemical histories are involved.

Based on this practical need, we propose here to study, through simulation and modeling, the curing of typical SBR and NBR samples in the oscillating bicone cell shown in Figure 1. This proposal presents challenging problems of fundamental aspects that have not been considered enough in the literature. They are concerned mainly with the knowledge of how the dynamic viscosity η' and the storage modulus G' vary with temperature T and the degree of vulcanization α along time t. In this sense, we believe that any effort to obtain a model supported on fundamental equations will be of significant value to users of these apparatus.

In the next sections, kinematic and dynamic aspects of the cell are first studied from the rheological point of view in order to define torque $M(t)$, shear stress $\tau(t)$, and shear rate $\dot{\gamma}(t)$ in relation to the proposed geometry. Then, the heat-transfer mechanisms in this cell are considered to evaluate the volumetric average temperature $[T]$ as function of time. The resulting equations must be solved by postulating the thermokinetic rheology of rubber compounds. Finally, we validate our model by comparison of theoretical predictions with experimental results obtained in the Monsanto rheometer MDR 2000.

THEORETICAL CONSIDERATIONS

The cone-plate geometry is a well-known cell in rheometry, and it has been rigorously studied for predicting rheometric functions of viscoelastic materials.[1-3] We consider here the bicone geometry shown in Figure 1, where the oscillating flow in spherical coordinates (ϕ, θ, r) is

$$v_\phi = W(t) r \frac{\left(\frac{\pi}{2} + \alpha_0 - \theta\right)}{2\alpha_0} \quad (1)$$

* To whom correspondence should be addressed.

Journal of Applied Polymer Science, Vol. 56, 967–977 (1995)
 CCC 0021-8995/95/080967-11

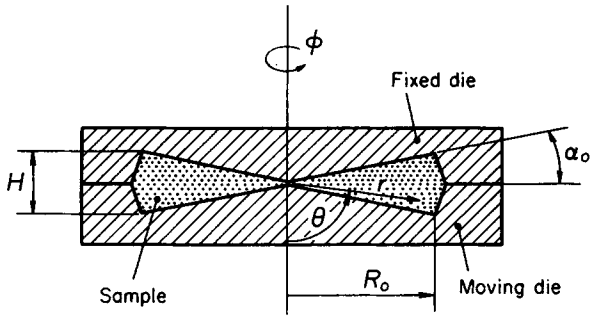

Figure 1 Sketch of the oscillating bicone cell. The spherical coordinate system (ϕ, θ, r) places a point in the sample. R_0, H, and α_0 are the cell dimensions (see Table I).

In eq. (1), $W(t) = W_0 \cos \omega t$ is the oscillating angular velocity. The shear rate is obtained as follows:

$$\dot{\gamma}(t) = -\frac{W(t)}{2\alpha_0} \tag{2}$$

and the evaluation of the total torque $M(t)$ yields

$$M(t) = K\tau(t) \tag{3}$$

where $K = \frac{2}{3}\pi R_0^3$.

The kinematics in the oscillating cell can be written as follows:

$$\dot{\gamma}(t) = -\dot{\gamma}_0 \cos \omega t \tag{4}$$

where ω is the oscillation frequency of the moving die and $\dot{\gamma}_0 = W_0/2\alpha_0$ is the maximum shear rate reached at each oscillation, which can be calculated from apparatus specifications (see Table I).

It is also simple to express at a given T and α the shear stress $\tau(t)$ through dynamic viscosities $\eta'(\omega) = G''(\omega)/\omega$ and $\eta''(\omega) = G'(\omega)/\omega$:

$$\tau(t) = \dot{\gamma}_0(\eta' \cos \omega t + \eta'' \sin \omega t) \tag{5}$$

The loss tangent can be written as

$$\tan \delta(\omega) = \frac{\eta'(\omega)}{\eta''(\omega)} = \frac{G''(\omega)}{G'(\omega)} \tag{6}$$

$G'(\omega)$ and $G''(\omega)$ are the storage and loss moduli, respectively. Therefore, from eq. (3), the total torque is

$$M(t) = K\dot{\gamma}_0(\eta' \cos \omega t + \eta'' \sin \omega t) \tag{7}$$

Table I Fixed Data for Numerical Simulation

Initial temperature (T_0)	=	298 K
Die temperature (T_h)	=	433 K
Oscillation frequency (ω)	=	10.47 s^{-1}
Strain (γ_0)	=	0.07
Apparatus constant (K)	=	19.4 cm^3
Total volume of sample (V)	=	3.5 cm^3
Volume ratio (V'/V)	=	0.82
Cell radius (R_0)	=	2.09 cm
Cone angle (α_0)	=	0.061 rad
Maximum gap (H)	=	0.27 cm

This torque can be decomposed into two parts:

$$S''(t) = K\dot{\gamma}_0\eta' \cos \omega t \tag{8}$$

and

$$S'(t) = K\dot{\gamma}_0\eta'' \sin \omega t \tag{9}$$

In general, rheometers report the maximum values of each periodic torque.

Since the temperature of the sample changes due to the exothermal curing reaction, we evaluate the volume-average temperature $[T]$ through the following macroscopic energy balance:

$$\rho V C_v \frac{d[T]}{dt} = h(\alpha)A(T_h - [T]) + \rho V Q_\infty \frac{d\alpha}{dt} + V'[\Phi] \tag{10}$$

which must be analyzed at each term. The left-hand side of this equation is the rate of heat stored in the sample with volume V, density ρ, and heat capacity C_v. According to the data reported in the literature,[4] we neglect the effect of temperature on ρ and C_v. In fact, the expansion coefficient β and the first derivative of the heat capacity with temperature ($\partial C_v/\partial T$) are of the order of 10^{-3} for compounds and vulcanizates when units are K^{-1} and J/g K^2, respectively. On the other hand, when the sample evolves

Table II Conventional Formulations[a] of SBR and NBR

Rubber	100.00	100.00
Zinc oxide	3.00	3.00
Sulfur	1.75	1.50
Stearic acid	1.00	1.00
Oil furnace black	50.00	40.00
TBBS[b]	1.00	0.70

[a] Nos. in the table are quantity-parts by mass.
[b] TBBS = *N-tert*-butyl-2-benzothiazole sulfenamide.

Table III Molecular and Rheological Parameters of Rubber Samples

Formulated Sample	Polymer	M_n (g/mol)	P_O	G_N^0 (Pa)	$G'_F = S'_F/K\gamma_0$ (Pa)
S1	SBR 1712	240,000	1.73	4.69×10^5	8.41×10^5
S2	SBR 1502	226,800	1.70	8.02×10^5	12.21×10^5
S3	NBR	96,900	1.57	6.01×10^5	11.73×10^5
S4	NBR	70,100	1.75	10.28×10^5	6.18×10^5

from the compounding state ($\alpha = 0$) to vulcanizate ($\alpha = 1$),[4] ρ increases around 5% while C_v decreases around 3%. This implies that ρC_v can be assumed independent of α by neglecting small quadratic terms.

The first term of the right-hand side in eq. (10) accounts the heat incorporated to the sample through the total area A. Also, it is assumed that the cavity walls are kept at constant temperature T_h. One should observe that $h(\alpha)$ is the heat-transfer coefficient that depends on physical properties of the sample, flow dynamics, temperature, and degree of vulcanization α. We propose here, as a first approximation,

$$h(\alpha) = h_0(1 + C\alpha) \tag{11}$$

Thus, in general, h may increase linearly with the molecular crosslinking through the conductivity of polymer matrix, as reported in the literature.[5] Therefore, we place h_0 and C as parameters to be fitted in the simulation process, as described later. According to our calculations, the heat-transfer coefficient can increase around 15–25% due to the crosslinking reaction (see Table V).

The second term of the right-hand side in eq. (10) considers the heat generated by the curing reaction.

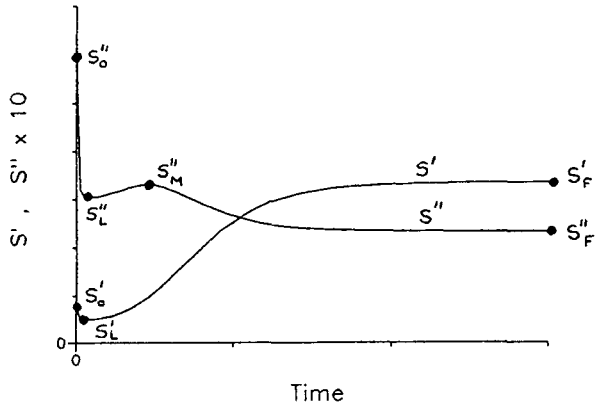

Figure 2 Typical vulcanization rheogram of rubber compounds obtained in the MDR 2000 rheometer. Dots indicate specific values of S' and S'' used in the fitting algorithm.

In this term, the degree of vulcanization is defined $\alpha = Q(t)/Q_\infty$, where Q_∞ is the total heat of the reaction and $Q(t)$ is the heat evolved until time t.[6]

The last term in the energy balance includes heat generation through viscous dissipation. This term is proportional to volume V', where the sample is subjected to deformation. One should observe that, usually, rheometers for rubber compounds have $V > V'$, because several grooves are machinated to catch the sample, in order to avoid slip of this sample on the die walls. Also, from the kinematics of the rheometric cell, one obtains

$$[\Phi] = \dot{\gamma}_0^2(\eta'\cos^2\omega t + \eta''\sin\omega t\cos\omega t) \tag{12}$$

Equation (12) is easily averaged in volume, because $\dot{\gamma}$ and τ are spatially constant throughout the cell.

We also need a kinetic expression describing the crosslinking reaction along time t. Despite the practical interest of accelerated sulfur vulcanization of rubber compounds, up to the present, there is not available a complete kinetic model that can predict the reactant concentration changes.[7–9] Nevertheless, recent experimental works[10–12] that follow the evolution of reactants along the vulcanization process with the help of high-performance liquid chromatography (HPLC) have given relevant results to elucidate the chemical steps involved in a possible kinetic mechanism.

According to the conventional compounding formulations used in this work (see Table II) and results described in the above-mentioned references,[11,12] one can imagine the accelerated sulfur vulcanization of rubbers as a sequence of chemical reactions in series. The first step is the scission of the octect sulfur ring (S_8) with the generation of various accelerator complexes, the evolutions of which are still open to debate.[10] Nevertheless, the consensus to date is that an intermediate species is formed where polysulfides and split parts of the accelerator are attached to the zinc atom of the zinc oxide used in the compound formulation (see Table II). Thus, after the first step, one can find intermediate species composed of *N-tert*-butyl-2-benzothiazole sulfenamide (TBBS),

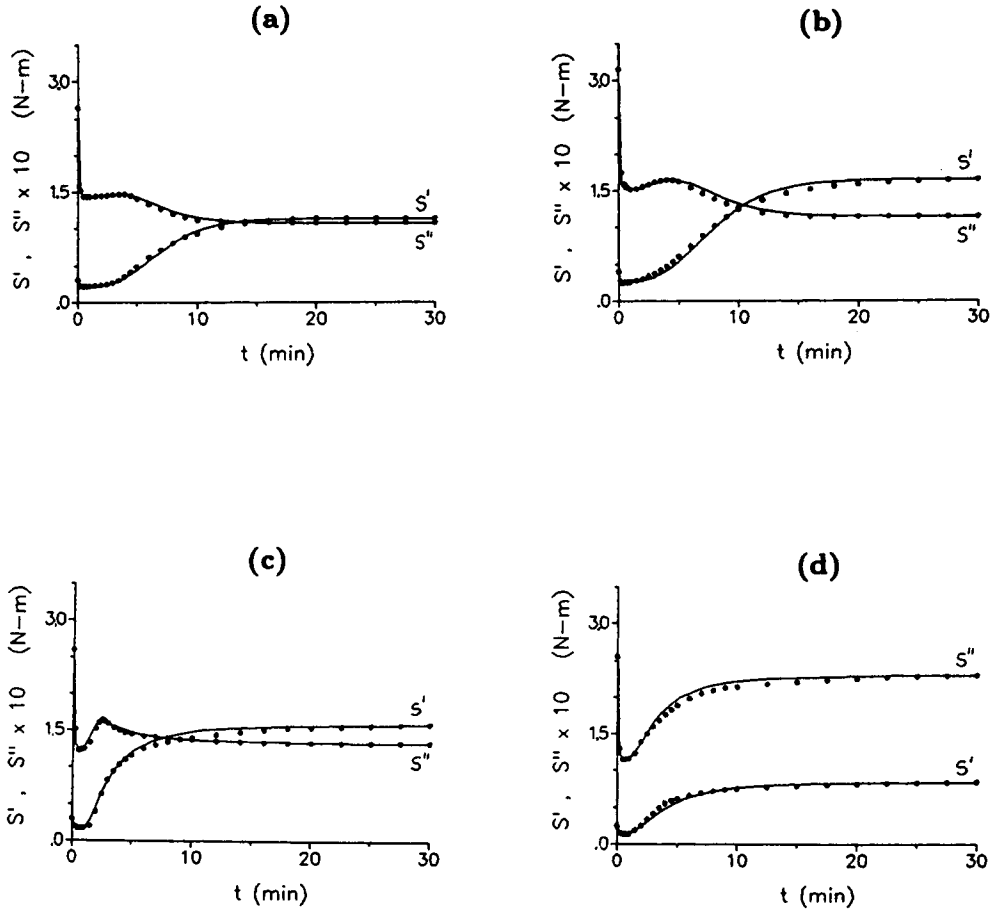

Figure 3 Comparison between (dots) experimental points and (full lines) model predictions for SBR and NBR samples: (a) S1; (b) S2; (c) S3; (d) S4 (see also Table III).

accelerator–zinc complexes, and sulfur. The second step consists in the formation of benzothiazole polysulfides (Bt–S_x–Bt, where $x \leq 4$ when the temperature is around 160°C). It is observed that the TBBS decreases by following a first-order chemical reaction while the decay in sulfur concentration is more compatible with a slow second-order chemical reaction. The third step is the conversion of Bt–S_x–Bt and the double bonds of the rubber matrix into an intermediate of the type rubber–S_x–Bt and the final crosslinks like rubber–S_x–rubber (for high temperature, the links between rubber chains are preferentially sulfide and bisulfides). There is also a certain amount of intramolecular crosslink with formation of a cyclic structure. In addition, HPLC results show that Bt–S_2–Bt reaches a maximum value at intermediate times, indicating that this species effectively follows the mechanisms of chemical reactions in series and it is the most important intermediate polysulfide of the type Bt–S_x–Bt. The steps thus described are consistent with the mechanism proposed by Coran,[13] where the sulfur vulcanization consists of predominantly three reactions in series that lead to final crosslinks and a parallel reaction that regenerates the precursor to crosslinks. A similar generalization mechanism is proposed by Morrison and Porter.[14]

Unfortunately, one has to conclude in relation to this aspect that, to date, there is not available values of the kinetic constants involved in these chemical reactions, despite the important progress obtained in order to understand the most probable chemical steps. Therefore, to proceed with our model that describes the vulcanization in the bicone cell, we decided to use a global kinetic model that allows us to evaluate the degree of vulcanization α described above in the energy balance. Of course, one shall not lose the direct relation between α and the concentration changes in the cell. This aspect is analyzed in the next sections.

According to the above discussion and to recent publications,[15–17] we propose that

$$\frac{d\alpha}{dt} = k\alpha^m(1 - \alpha)^n \tag{13}$$

Table IV Kinetic Parameters of Vulcanization

Sample	k_0 (1/s)	E (J/mol)	Q_∞ (J/g)	t_0 (s)	$\hat{T}_0$ (K)	m	n
S1	4.0×10^8	8.9×10^4	0.45×10^2	6.0×10^{-14}	1.5×10^4	0.50	1.00
S2	3.3×10^8	8.9×10^4	0.50×10^2	2.5×10^{-14}	1.5×10^4	0.50	1.00
S3	6.4×10^8	8.9×10^4	3.50×10^2	2.0×10^{-15}	1.5×10^4	0.50	1.30
S4	6.2×10^8	9.0×10^4	3.50×10^2	2.2×10^{-15}	1.5×10^4	0.45	1.25

where m and n are parameters that depend on the mechanisms of the curing reaction. In eq. (13), k is the Arrhenius constant. Thus,

$$k = k_0 \exp\left(-\frac{E}{R[T]}\right) \tag{14}$$

where E is the activation energy and k_0 is the preexponential constant.

The initiation of the covalent crosslinks of polymer chains requires an induction time[6] which can be expressed as

$$\bar{t} = \int_0^t \frac{dt}{t_0 \exp(\hat{T}_0/[T])} \tag{15}$$

where t_0 and $\hat{T}_0$ are kinetic constants that depend on the type of rubber compound. If $\bar{t}$ is less than 1, the curing reaction is quenched; otherwise, the degree of vulcanization α starts to evolve according to eq. (13).

To complete the formulation of the model, we need to express η' and G' as functions of α and $[T]$. After compiling relevant information concerning the change of these rheometric functions within the context of linear viscoelasticity, we propose that

$$\eta' = \eta'(T_0) \exp\left(\frac{\Delta H''}{R} \frac{(T_0 - [T])}{T_0[T]}\right) \times \exp(C_1\alpha + C_2\alpha^2) \tag{16}$$

and

$$G' = G'(T_0)\left(\frac{[T]}{T_0}\right)^\alpha \times \exp\left(\frac{\Delta H'}{R} \frac{(T_0 - [T])}{T_0[T]} (1 - \alpha)\right) \exp(C_3\alpha) \tag{17}$$

where $\eta'(T_0)$ and $G'(T_0)$ are evaluated at the reference temperature T_0 when $\alpha = 0$ and at frequency ω (around 10.47 rad/s for the MDR 2000).

Equation (16) considers the classical exponential term that allows the dynamic viscosity to decrease with $[T]$. In addition, the effect of curing is accounted for through two mechanisms. One evaluates the change of the activation energy with α; thus,

$$\Delta H'' = \Delta H''_v \alpha + \Delta H''_f (1 - \alpha) \tag{18}$$

where it is clear that the activation energy of the vulcanized rubber ($\alpha = 1$) is different from that of the uncrosslinked compound ($\alpha = 0$). The other considers the evolution of η' on pure kinetic aspects. In fact, even at $[T]$ = constant, η' shall change with α. We find that this last dependence of the dynamic viscosity may involve a rather complex function of α in the exponential part, and it is discussed later.

The storage modulus G' changes with temperature through two factors: The term $([T]/T)^\alpha$ is consistent with the rubber elasticity theory for crosslinked networks[18,19] and the exponential term involving $[T]$ and α corresponds to the fluid response of samples.

Table V Heat Transfer and Thermokinetic Parameters

Sample	h_0 (W/m^2 K)	C	$\frac{\Delta H''_f}{R}$ (K)	$\frac{\Delta H'}{R}$ (K)	C_1	C_2	C_3
S1	1.61×10^2	0.15	5.83×10^2	3.28×10^2	−0.148	−0.44	0.93
S2	1.61×10^2	0.15	6.96×10^2	4.30×10^2	0.144	−0.79	1.05
S3	1.61×10^2	0.20	7.08×10^2	5.37×10^2	0.689	−0.98	1.30
S4	1.61×10^2	0.25	7.61×10^2	5.61×10^2	0.295	0	0.84

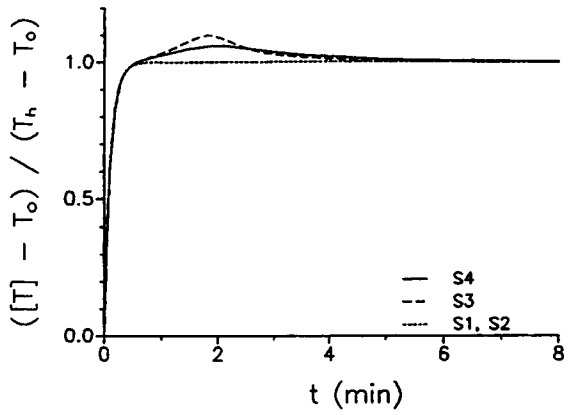

Figure 4 Dimensionless volume-average temperature of samples $([T] - T_0)/(T_h - T_0)$, as function of time t. T_0 is the initial temperature of samples, and T_h, the vulcanization temperature imposed on the dies. Samples are the same as in Figure 3.

In this context of analysis, the effective activation energy $\Delta H'(1 - \alpha)$ shows us that for $\alpha = 1$ the sample evolves thermically according to the rubber elasticity theory only. Since the storage modulus also changes with α when $[T]$ = constant, an additional term in eq. (17) presents the typical exponential growth of sample elasticity when the degree of vulcanization increases. The model described through eqs. (1)–(18) is solved numerically by standard methods of coupled ordinary differential equations (see, e.g., Carnahan et al.[20]).

EXPERIMENTAL

Experiments are carried out in the Moving Die Rheometer MDR 2000. Samples are formulated with commercial SBR and NBR (see Table II for conventional formulations). These samples are designated S1–S4, as shown in Table III. The molecular parameters included in this table are estimated with the rheometric molecular weight distribution technique described in the literature.[21,22] This technique uses experimental data of the storage modulus of polymer melts in the terminal and plateau zone of linear viscoelasticity. In Table III, the approximate values of average molecular weight M_n, polydispersity Po, and plateau modulus G_N^0 correspond to unformulated polymers.

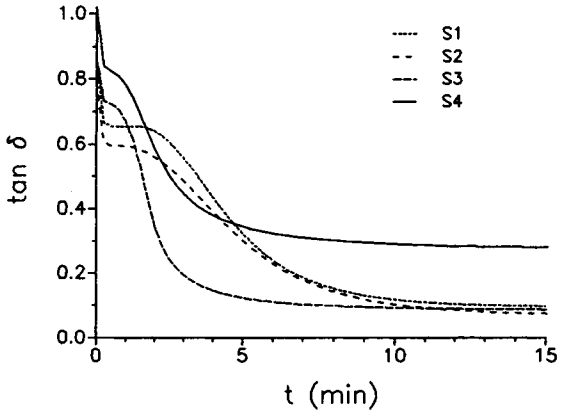

Figure 5 Loss tangent tan δ, as function of time t. Samples are the same as in Figure 3.

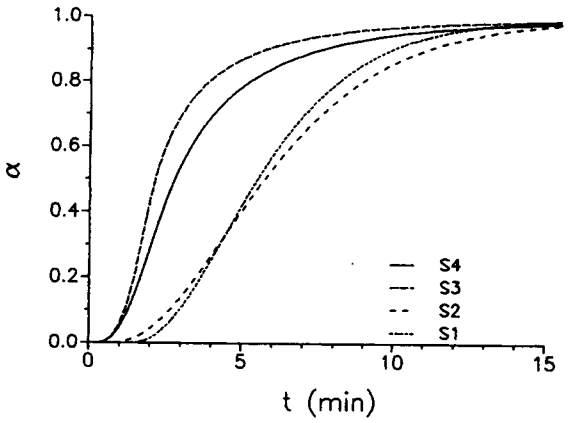

Figure 6 Degree of vulcanization α, as function of time t. Samples are the same as in Figure 3.

The dies are set at 160°C. The torques S' and S'' measured in the apparatus, are related to rheometric functions through eqs. (8) and (9), evaluated at the maximum values. A typical rheogram obtained in the MDR 2000 is shown in Figure 2, where specific values of S' and S'' used in the fitting algorithm are pointed out (see Appendix).

RESULTS AND DISCUSSION

Experimental results of the four samples tested in the MDR 2000 are simulated with the proposed model [eqs. (1)–(18)] through the strategy for fitting parameters, described in the Appendix. In general, we have been able to fit experimental points with enough accuracy and to determine the model constants $\{h_0, C, C_1, C_2, C_3, \Delta H_v'', \Delta H_f'', \Delta H', k_0, E, Q_\infty, \hat{T}_0, t_0, m, n\}$. Results are summarized in Figure 3 and Tables IV and V. One should also observe that there are fixed data in the simulation, which are initial temperature T_0, die temperature T_h, oscillation frequency ω, strain γ_0, apparatus constant K, sample volumes V and V', and geometric parameters (see Table I).

Figure 3 shows in full lines the simulation of rheograms, and one sees that the model reproduces well experimental points. At low times, the torques

S' and S'' present a sharp decrease because the samples are under rapid heating. Since the heat transfer is efficient in the MDR 2000, the samples reach a temperature close to T_h in a few seconds. Then, these torques stay almost constant because there are neither thermal changes nor final crosslinks during a short period of time. In fact, the samples are reaching the induction time required to start the curing reaction, as described in eq. (15). At higher times, Figure 3 shows substantial variations of the torques, because the crosslinking of chains modify the mechanical response of rubber compounds. Once more, the energy balance is relevant here to describe this phenomenon as shown, for instance, in Figure 4, where samples S3 and S4 present a clear overshooting in the temperature evolution. This indicates that the dies take heat when the exothermal reaction is relatively intensive.

The increase of the degree of vulcanization strongly affects the loss tangent as shown in Figure 5. Thus, tan δ decreases after the curing reaction is ignited. This is consistent with the fact that the vulcanized material dissipates the oscillating strain much less than does the corresponding rubber compound.

Figure 6 shows the evolution of the degree of vulcanization, where one can determine the time at which the curing reaction is ignited. These times are around 2 min for SBR (S1, S2) and 1 min for NBR (S3, S4). In Figure 7, we report $d\alpha/dt$ as a function of time to visualize the maximum reaction rate and the time of reaction extinction where $\alpha \approx 1$. For NBR, the maximum value of the reaction rate is observed around $t = 2$ min, and for SBR, this point is reached approximately at $t = 4$ min. The peaks of the reaction rate of NBR are substantially greater than are those of SBR samples.

Values of Q_∞ in Table IV indicate that NBR yields more heat than does SBR during the vulcanization process (see temperature overshooting in Fig. 4). Also, the values of the kinetic constant t_0 for S3 and S4 are lower than those of S1 and S2, and this is also depicted in Figure 6, where one can determine the ignition times. Thus, by decreasing t_0, the ignition time also decreases. Table IV shows that NBR has high values of k_0 in relation to SBR, and this is compatible with reaction rates depicted in Figure 7.

It is also important to analyze the values assigned to m and n in eq. (13). When S' increases sharply at the onset of vulcanization, m shall be low. After the inflexion point of S', the rate at which S' tends to S'_F depends on n. Thus, we required relatively high values of n for S3 and S4 because NBR samples tend slowly to S'_F.

From the analysis of reactant evolutions in accelerated sulfur vulcanization[11,12] and the predictions of our model, several conclusions can be obtained. In fact, the small values of the kinetic constant t_0 for NBR are directly associated to a rapid generation of the intermediate NBR–S_x–Bt from Bt–S_x–Bt during the induction time, and this may be due to two reasons: (1) The strong tendency of the group —C≡N in the copolymeric part of the NBR to be an electron donor, which makes the double bonds of the polybutadiene copolymer more reactive. One should observe that this macromolecular part in the SBR is composed of rather inert and nonpolar benzene groups. (2) There is a steric effect of the polystyrene part on the reactivity of double bonds of the SBR. This effect is minimized in the case of the NBR, and, hence, the double bonds of the polybutadiene copolymer are more exposed to the reaction.

Moreover, since n, k_0, and Q_∞ are higher for NBR than for SBR samples (see Table IV) and the ignition point in our model is associated to the onset of final crosslink generation of the type rubber–S_x–rubber, one finds quantitative reasons to assign more reactivity to NBR than to SBR during the transformation of rubber–S_x–Bt to the final network. We can reach an important conclusion here based on the values of t_0, n, k_0, and Q_∞. Thus, the chemistry of the rubber used in the compound formulation affects significantly the rate of vulcanization, and, hence, a kinetic mechanism for accelerated sulfur vulcanization of rubber copolymers shall be established by considering explicitly the role of the copolymer associated to the polybutadiene part, i.e., to specify the concentration of rubber double bonds in the mechanism steps is not enough if differences in induction times and kinetic constants must be explained.

Further explanations on the kinetic mechanisms that make differences in reactivity between SBR and NBR are still under research, and one of the reasons

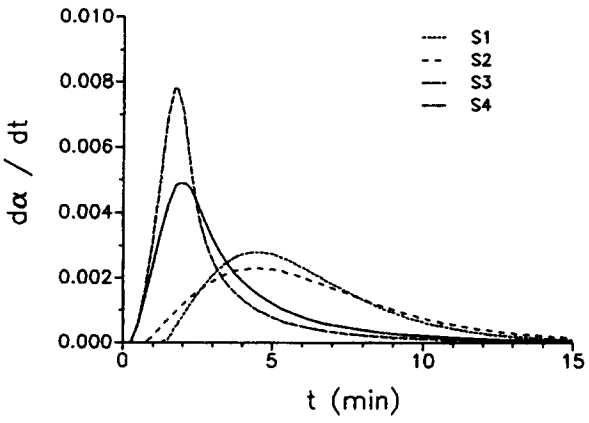

Figure 7 Reaction rate $d\alpha/dt$, as function of time t. Samples are the same as in Figure 3.

Table VI Ratios Between Characteristic Torques S' and S''

Sample	C_3	S'_F/S'_O	$C_1 + C_2$	S''_F/S''_O	$\Delta H''_f/R$	S''_L/S''_O	$\Delta H'/R$	S'_L/S'_O
S1	0.93	3.68	−0.59	0.41	583	0.54	328	0.71
S2	1.05	4.15	−0.65	0.36	696	0.48	430	0.64
S3	1.30	5.31	−0.29	0.51	708	0.47	537	0.57
S4	0.84	3.36	0.29	0.90	761	0.45	561	0.55

for this situation is that it is not well understood if accelerated sulfur vulcanization is carried out by free-radical or polar mechanisms;[10] it is now believed that both mechanisms are present.[23] It has also to be pointed out that the torques S' and S'' are only sensitive to the final steps of the vulcanization process, where crosslinks of polymer chains become effective. In the first steps, chemical changes occur only for small molecular weight species (sulfur, TBBS, etc.) without any substantial effect on the rheological properties like dynamic moduli.

From Table V, one can readily conclude that the constant C_3 is related to the experimental ratio $S'_F/S'_O = G'_F/G'_O$ [see Table VI and eq. (A.4)]. Physically, this means that C_3 obtained from the fitting procedure allows us to quantify the elasticity increase of rubber compounds ($\alpha = 0$) due to vulcanization ($\alpha = 1$).

Also, the sum of the constants C_1 and C_2 is related to the evolution of the dynamic viscosity due to both temperature and degree of vulcanization. In fact, this value correlates with the experimental ratio $S''_F/S''_O = \eta'_F/\eta'_O$ as shown in Table VI. Of course, this is only true when $\Delta H''_v$ does not change significantly in the samples to be compared [see eq. (A.3)].

Table VI also shows that the activation energy $\Delta H''_f$ is related to the thermal decay of dynamic viscosity and correlates with the experimental ratio $S''_L/S''_O = \eta'_L/\eta'_O$ [see eq. (A.1)]. Similarly, $\Delta H'$ describes the thermal decay of the storage modulus and correlates with the experimental ratio $S'_L/S'_O = G'_L/G'_O$ [see eq. (A.2)].

One can observe that rheograms may present a relative maximum for S'', which is designated here S''_M [see also eq. (A.5)]. This, of course, requires a physical interpretation that is not simple to infer. We discuss one possible mechanism that may generate this maximum value. Thus, at short times, one can imagine the sample as a compound where the polymer chains are entangled as far as the average molecular weight M_w is greater than the critical molecular weight $M_c \approx \rho RT/G^0_N$. In addition, chains may be chemically and physically bounded to the carbon black particles if the incorporation and dispersion processes are effective with little mechanical degradation.[24] Under these circumstances, it is well known from mechanical spectrometry that G'' and G' present a crossover at a relatively low frequency when $\alpha = 0$. After the crossover, G'' may be either a slowly monotonic increasing function toward the transition zone (for relatively low M_n and high polydispersity Po) or may, however, present a maximum value followed by a minimum, after which the transition zone is expected (for very high M_n and low P_o). Within the context of molecular theories,[25] chains are in the reptational zone under these situations. Therefore, for the frequency of the MDR 2000 (around 10.47 rad/s), one can expect that at the onset of vulcanization the polymer matrix presents predominantly entanglements and that the first crosslinks have the effect of increasing the average molecular weight. Thus, G'' may present the maximum value for some period of time (behaving as a sample of high M_n and low Po) until the number of crosslinks is high enough to screen out the entanglements and, hence, reptational relaxations cancel out.[18] At this moment, the value of G'' shall decrease because the sample is behaving as an elastic solid. Some validation of this idea is precisely found in the response of sample S4, which does not present the relative maximum in S'' (it is the counterexample). This seems reasonable in relation to the above discussion since this sample has the lower average molecular weight and a relatively high polydispersity. Thus, the first crosslinks are not able to increase M_n enough before the entanglements are being screened out. To reinforce this idea, one should observe Figure 5, which depicts the evolution of tan δ with time. In this figure, the loss tangent decreases slowly when S'' is around the maximum; the decrease is a consequence of the increase of S', predominantly.

To conclude in this aspect, we believe that the plateau of the loss tangent around the onset of vulcanization (see Fig. 5) is due to the competition of two different modes of relaxation. When entanglements predominate, chains are reptating. On the other hand, when covalent crosslinks screen out entanglements, the material relaxes as a viscoelastic solid. Thus, increasing the degree of vulcanization, S'' shall tend to zero at around the frequency of the

MDR 2000. The plateau is more evident when M_n is high and the polydispersity is low. One should also observe that the effect of oil in sample S1 (SBR 1712 is plasticized with around 25% by weight of oil) is to increase the effect of dissipation (see Tables II and III). This discussion requires, of course, additional experimentation of well-characterized samples, either in the mechanical spectrometer and the MDR 2000.

Another interesting aspect of this subject is the connexion of S'_F with molecular parameters M_n and Po. Table III presents the plateau modulus G^0_N of the unformulated polymers (reference temperature is 160°C) and the vulcanizate modulus G'_F, which is obtained from S'_F at the frequency of the MDR 2000. It is clear that there is not a direct relation between G^0_N and G'_F as one may be motivated to find it. However, M_n and Po have an important role in the value of G'_F, which is predominantly a result of the interplay between molecular parameters and the mechanism of reaction. In fact, a comparison of S3 and S4 shows that for high M_n and low Po the resulting G'_F should be higher. This is so because from the rubber elasticity theory[19] equation $G'_F \approx \nu RT(1 - 2M_c/M_n)$ is satisfied, ν being the number of strands per cubic centimeter. Thus, for a fixed number of crosslinks, ν increases more if M_n is high and the sample is monodisperse. To reinforce this conclusion, one can observe that the differences in M_n and Po for S3 and S4 are around 27 and 10%, respectively. The sum of both effects produces a high difference in G'_F of these samples.

The above discussion cannot be applied directly to SBR samples. In fact, since S1 and S2 have almost the same polydispersity and similar average molecular weights (difference is around 5.5%), one may be induced to conclude that both samples have almost the same G'_F. However, S1 is plasticized with oil (the polymer is SBR 1712) and this has a strong incidence in reducing the value of storage modulus $G'(\omega)$. Finally, the higher value of tan δ when $\alpha = 1$ corresponds to sample S4, and this is compatible with its molecular parameters (low M_n and high Po) and the previous discussion.

CONCLUSIONS

This work presents a model that allows us to simulate the curing curves of SBR and NBR in the Monsanto Rheometer MDR 2000. We can estimate kinetic and thermorheological parameters. Thus, it is possible to find the dependence of the reaction rate and the rheometric functions (dynamic viscosity and storage modulus at the frequency of the apparatus) with temperature and degree of vulcanization. Also, we find relationships involving torques S' and S'' at different times of the curing process that correlate directly with changes of dynamic rheometric functions.

Several conclusions are obtained on the interplay between rheological and molecular parameters, showing that further research on the subject has a promising utility in the characterization and quality control of rubber products. Future research should be directed to a better understanding and prediction of reactant concentration changes during the accelerated sulfur vulcanization of rubber copolymers.

NOMENCLATURE

A	total heat-transfer area (m^2)
C	heat-transfer parameter [eq. (11)]
C_i	thermorheological parameters [i = 1, 2, 3; eqs. (16) and (17)]
C_v	sample heat capacity (J/g K)
E	kinetic activation energy (J/mol)
G'	storage modulus (Pa)
G''	loss modulus (Pa)
$\Delta H'$	activation energy of the storage modulus (J/mol)
$\Delta H''_f$	activation energy of the compound dynamic viscosity (J/mol)
$\Delta H''_v$	activation energy of the vulcanizate dynamic viscosity (J/mol)
$\Delta H''$	$\alpha\ \Delta H''_f + (1 - \alpha)\ \Delta H''_v$ (J/mol)
h	heat-transfer coefficient (W/m^2 K)
h_0	heat-transfer coefficient before the vulcanization onset (W/m^2 K)
K	apparatus constant (see Table I)
k	kinetic Arrhenius constant (s^{-1})
k_0	preexponential factor of the kinetic Arrhenius constant (s^{-1})
$M(t)$	total torque on the sample (N-m)
m	kinetic parameter [eq. (13)]
n	kinetic parameter [eq. (13)]
$Q(t)$	heat of vulcanization reaction evolved to time t (J/g)
Q_∞	total heat of vulcanization reaction (J/g)
R	universal gas constant (J/mol K)
R_0	rheometric cell radius (m)
r	spherical radial coordinate (m)
S'	elastic torque on the sample (N-m)
S''	viscous torque on the sample (N-m)
S'_O	initial elastic torque (N-m)
S'_L	minimum elastic torque before the vulcanization onset (N-m)

S'_F final elastic torque ($\alpha = 1$) (N-m)
S''_O initial viscous torque (N-m)
S''_L minimum viscous torque before the vulcanization onset (N-m)
S''_M viscous torque peak after the vulcanization onset (N-m)
S''_F final viscous torque ($\alpha = 1$) (N-m)
T sample temperature (K)
T_h die temperature (K)
$\hat{T}_0$ kinetic constant to define the vulcanization induction time [eq. (15)] (K)
t time (s)
t_0 kinetic constant to define the vulcanization induction time [eq. (15)] (s)
$\bar{t}$ dimensionless induction time
V dimensionless induction time
V total sample volume (m^3)
V' sample volume subjected to deformation (m^3)
v_ϕ sample angular velocity component in the rheometric cell (m/s)
$W(t)$ oscillating angular velocity of lower die (see Fig. 1) (rad/s)
W_0 maximum value of oscillating angular velocity of lower die (rad/s)

Greek Symbols

α degree of vulcanization, defined as $Q(t)/Q_\infty$
α_0 cone angle of rheometric cell (see Table I) (rad)
γ_0 maximum shear deformation of sample
$\dot{\gamma}_0$ maximum shear rate (s^{-1})
$\dot{\gamma}(t)$ time dependent shear rate (s^{-1})
η' dynamic viscosity (Pa-s)
η'' G'/ω (Pa-s)
θ azimutal spherical coordinate
ϕ angular spherical coordinate
ρ sample density (g/m^3)
$\tau(t)$ time-dependent shear stress (Pa)
$[\Phi]$ volume average energy dissipation (W/m^3)
ω oscillation frequency of lower die (rad/s)

The authors wish to acknowledge the financial aid received from CONICET (Consejo Nacional de Investigaciones Científicas y Técnicas de Argentina) and from UNL (Universidad Nacional del Litoral, Santa Fe, Argentina). The rubber samples provided by PASA (Petroquímica Argentina S.A.) are highly appreciated.

APPENDIX: STRATEGY FOR FITTING PARAMETERS

The model has a set of undetermined parameters which are $\{C_1, C_2, C_3, C, \Delta H''_v, \Delta H''_f, \Delta H', h_0\}$. Also, the cure kinetic parameters $\{k_0, E, \hat{T}_0, t_0, Q_\infty, m, n\}$ can be assigned a priori from the literature data[6,15] and then corrected slightly in the fitting strategy according to the particular characteristics of each sample. Additionally, we determine geometric and dynamic parameters from apparatus specifications (see Table I and Fig. 1) used in the experimental part. Physical properties ρ and C_v are obtained from standard handbooks.[4] Therefore, in the fitting procedure, we use specific values of torques S' and S'' as illustrated in Figure 2. These torques can be converted through eqs. (8) and (9) to either dynamic moduli $\{G'_O, G''_O, G'_L, G''_L, G'_F, G''_F, G''_M\}$ or corresponding dynamic viscosities.

Since at S''_L and S'_L the cure reaction is not ignited ($\alpha = 0$), from eqs. (16) and (17), we determine

$$\frac{\Delta H''_f}{R} = \frac{T_0 T_h}{(T_h - T_0)} \ln\left(\frac{S''_O}{S''_L}\right) = \frac{T_0 T_h}{(T_h - T_0)} \ln\left(\frac{\eta'_O}{\eta'_L}\right) \quad \text{(A.1)}$$

and

$$\frac{\Delta H'}{R} = \frac{T_0 T_h}{(T_h - T_0)} \ln\left(\frac{S'_O}{S'_L}\right) = \frac{T_0 T_h}{(T_h - T_0)} \ln\left(\frac{G'_O}{G'_L}\right) \quad \text{(A.2)}$$

When the curing reaction is completed ($\alpha = 1$),

$$C_1 + C_2 + \frac{\Delta H''_v}{R} \frac{(T_0 - T_h)}{T_0 T_h} = \ln\left(\frac{S''_F}{S''_O}\right) = \ln\left(\frac{\eta'_F}{\eta'_O}\right) \quad \text{(A.3)}$$

and

$$C_3 = \ln\left(\frac{S'_F T_0}{S'_O T_h}\right) = \ln\left(\frac{G'_F T_0}{G'_O T_h}\right) \quad \text{(A.4)}$$

Another condition can be deduced when S'' presents a maximum value. Thus, after imposing $(dS''/dt) = 0$ in eq. (16), one obtains

$$C_1 + 2C_2\alpha_M + \left(\frac{\Delta H''_v}{R} - \frac{\Delta H''_f}{R}\right) \frac{(T_0 - T_h)}{T_0 T_h} = 0 \quad \text{(A.5)}$$

as far as $[T] \approx$ constant. We find that this is a good approximation, due to the very fast thermal recovery in the MDR 2000. In eq. (A.5), α_M is the degree of vulcanization where S'' is maximum. From eqs. (A.3), (A.5), and (16) evaluated at α_M, we solve the algebraic system in order to evaluate $\hat{C}_1$, C_2, and α_M. Here, we define $\hat{C}_1 = C_1 + \Delta H''_v(T_0 - T_h)/RT_0T_h$. In addition, $\Delta H''_v/R$ could be estimated from the repetition of the MDR 2000 test on the vulcanized sample ($\alpha = 1$) at two different temperatures; however, we determined it by trial and error ($\Delta H''_v$ is around $\Delta H''_f/2$). It has to be mentioned here that some sam-

ples do not present the maximum [see Fig. 3(d)]. In this particular case, eq. (A.5) is not needed, because it is also true that $C_2 = 0$.

Finally, h_0 is estimated from eq. (10) at small times. Thus, before the onset of vulcanization ($\alpha = 0$) and since $[\Phi]$ is negligible in comparison to the heat transfer during this period of time, the energy balance reduces to

$$\rho V C_v \frac{d[T]}{dt} = h_0 A(T_h - [T]) \tag{A.6}$$

the solution of which is

$$\frac{T_h - [T]}{T_h - T_0} = e^{-(h_0 A/\rho V C_v)t} \tag{A.7}$$

This equation can be used to fit experimental data at small times in order to determine h_0.

REFERENCES

1. K. Walters, *Rheometry,* Chapman and Hall, London, New York, 1975, Chaps. 4 and 6.
2. R. B. Bird, R. C. Armstrong, and O. Hassager, *Dynamics of Polymeric Liquids,* Wiley, New York, 1977, Chap. 4.
3. W. R. Schowalter, *Mechanics of Non-Newtonian Fluids,* Pergamon Press, Oxford, 1978, Chap. 8.
4. J. Brandrup and E. H. Immergut, *Polymer Handbook,* 3rd ed., Wiley, New York, 1989, Section V.
5. M. R. Kamal and M. E. Ryan, in *Fundamentals of Computer Modeling for Polymer Processing,* C. L. Tucker III, Ed., Hanser, Munich, 1989.
6. A. I. Isayev, in *Comprehensive Polymer Science,* Allen and Bevington, Eds., Pergamon Press, Oxford, 1989, Vol. 7, Chap. 11.
7. F. W. Billmeyer, *Textbook of Polymer Science,* 2nd. ed., Wiley, New York, 1971, Chap. 19.
8. P. J. Flory, *Principles of Polymer Chemistry,* 9th ed., Cornell University Press, London, 1975, Chap. XI.
9. R. Taylor and P. N. Son, *Encyclopedia of Chemical Technology,* M. Grayson, Ed., 3rd ed., Wiley, New York, 1982, Vol. 20.
10. M. R. Krejsa and J. L. Koenig, *Rubber Chem. Technol.,* **66,** 376 (1993).
11. C. J. Hann, A. B. Sullivan, B. R. Host, and G. H. Kuhls, *Rubber Chem. Technol.,* **67,** 76 (1994).
12. A. B. Sullivan, C. J. Hann, and G. H. Kuhls, *Rubber Chem. Technol.,* **65,** 488 (1992).
13. A. Y. Coran, *Rubber Chem. Technol.,* **37,** 689 (1964).
14. N. J. Morrison and M. Porter, *Rubber Chem. Technol.,* **57,** 63 (1984).
15. K. Jönsson and P. Flodin, *J. Appl. Polym. Sci.,* **43,** 1777 (1991).
16. J. Burger, N. Burger, and M. Pogu, *Rubber Chem. Technol.,* **66,** 19 (1993).
17. J. S. Deng and A. I. Isayev, *Rubber Chem. Technol.,* **64,** 296 (1991).
18. J. D. Ferry, *Viscoelastic Properties of Polymers,* Wiley, New York, 1970, Chap. 14.
19. L. R. G. Treloar, *The Physics of Rubber Elasticity,* 3rd ed., Clarendon Press, Oxford, 1975, Chap. 4.
20. B. Carnahan, H. A. Luther, and J. O. Wilkes, *Applied Numerical Methods,* Wiley, New York, 1969, Chap. 6.
21. J. A. Deiber, M. B. Peirotti, and R. A. Bortolozzi, *J. Elast. Plast.,* **25,** 22 (1993).
22. W. H. Tuminello, *Polym. Eng. Sci.,* **26,** 1339 (1986).
23. A. Roychoudhury and S. K. De, *J. Appl. Polym. Sci.,* **50,** 811 (1993).
24. J. A. Deiber and D. Roig Fernández, *J. Elast. Plast.,* **23,** 239 (1991).
25. M. Doi and S. F. Edwards, *The Theory of Polymeric Dynamics,* Clarendon Press, Oxford, 1986, Chaps. 6 and 7.

Received March 2, 1994
Accepted November 16, 1994